Green Chemistry

Multicolor-Tunable Ultralong Room Temperature Phosphorescence Based on Cyclodextrin Metal-Organic Frameworks

Journal:	*Green Chemistry*
Manuscript ID	GC-ART-04-2025-001603.R1
Article Type:	Paper
Date Submitted by the Author:	23-May-2025
Complete List of Authors:	Zhang, Jiayin; Tianjin University Tang, Jiaxuan; Tianjin University Zhang, Yongsheng; Tianjin University Chen, Yifu; Peking University, Gong, Junbo; Tianjin University, Chemical Engineering

1. A series of multicolor persistent phosphorescent crystalline materials were constructed using the inherently green, heavy atom-free γ-cyclodextrin (γ-CD) metal-organic framework (CD-MOF) through guest encapsulation. These materials have the potential to replace traditional toxic heavy metals and petroleum-based polymers, thereby advancing green chemistry.

2. Quantitatively, the CD-MOF exhibits an ultralong phosphorescence lifetime (553 ms) without rare-earth metals, while qualitatively, it demonstrates recyclability, aqueous synthesis, and biocompatibility.

3. Future research could explore fully bio-sourced fluorescent dyes and mother liquor recycling options, which would promote the greenness of the product and reduce waste generation.

ARTICLE

Multicolor-Tunable Ultralong Room Temperature Phosphorescence Based on Cyclodextrin Metal-Organic Frameworks

Received 00th January 20xx,
Accepted 00th January 20xx

DOI: 10.1039/x0xx00000x

Jiayin Zhang,[a,c] Jiaxuan Tang,[a,c] Yongsheng Zhang,[a,c] Yifu Chen,[b*] Junbo Gong[a,c*]

A series of multicolor persistent phosphorescent crystalline materials were constructed using the inherently green, heavy atom-free *γ*-cyclodextrin (*γ*-CD) metal-organic framework (CD-MOF) through guest encapsulation. Attributed to the fact that macrocycles effectively suppress the aggregation of guests and form rigid environment via assembly with potassium ions, resulting in a lifetime and phosphorescence quantum yield of 553 ms and 8.19 %, respectively. Furthermore, upon encapsulation with commercial dyes such as sodium fluorescein (Flu) and Rhodamine B (RhB), full-color afterglow emissions were achieved through phosphorescence energy transfer. This work provides a universal method for designing and preparing environmentally friendly phosphorescence materials, overcoming the inherent limitations of degradation and recyclability in organic room-temperature phosphorescence (RTP) compounds.

1. Introduction

Room-temperature phosphorescent materials (RTP) have received significant attention due to their distinctive long emission lifetimes and large Stokes shifts.[1-3] Compared to inorganic phosphors, organic RTP materials offer advantages such as low cost, versatile molecular design, and environmental friendliness.[4-6] However, achieving RTP in organic materials at room temperature still faces several challenges because of the inherently weak spin-orbit coupling (SOC) or low intersystem crossing (ISC) process, as well as multiple deactivation pathways of organic molecules.[7-9] To address these challenges, several effective strategies have been developed to improve the performance of organic phosphorescence, including polymerization,[10-12] crystallization,[13-15] organic-inorganic hybridization[16-20]and supramolecular assembly.[21-24] Among these approaches, macrocycle-mediated host-guest interaction has emerged as a particularly promising platform, with cyclodextrins (CDs) demonstrating exceptional potential for constructing air-stable RTP systems.[25-27] CDs, are natural macromolecular oligosaccharide that are non-toxic, abundantly available, and can be degraded in the environment. They composed of *α*-(1,4)-linked glucopyranose units, mainly include *α*-, *β*-, and *γ*-CDs, which possess different numbers of glucose units (6, 7, and 8, respectively). Their well-defined hydrophobic cavity preferentially accommodates uncharged or negatively charged guests, thereby reducing molecular vibrations, rotations, and intercalations of the encapsulated phosphors while shielding them from environmental quenchers.[28, 29] As early as 1982, Turro and co-workers demonstrated a host-guest assembly-based RTP system by constructing 1-bromonaphthalene or 1-chloronaphthalene into *β*-CDs in a nitrogen-purged aqueous solution.[30] More recently, Li et al. reported an aqueous-phase ultralong RTP system derived from p-biphenyl boronic acid and *β*-CD.[21] Subsequently, Liu's group developed a *β*-CD-based supramolecular blue RTP material using terephthalic acid (PPA) as the guest molecule.[31] Given their biocompatibility and unique cavity structure, CD-based supramolecular architectures represent a sustainable pathway toward advanced luminescent materials. However, the host-guest systems based on CDs may still allow residual vibration/ rotation motions due to the dynamic supramolecular interactions and disordered packing, thereby limiting the phosphorescence efficiency.

Interestingly, the bidentate -OCCO- motifs present on the primary and secondary faces of CDs molecules provide an opportunity for building extended CDs metal-organic frameworks (CD-MOFs) through coordination with alkali or alkaline metal ions.[32] In contrast, CD-MOFs inherit the encapsulation capability of native CDs while introducing a rigid, crystalline framework that synergistically enhances spatial constraints, suppressing non-radiative pathways. [33, 34] The first CD-based MOF, *γ*-CD metal-organic framework (CD-MOF), was reported by Stoddart et al.in 2010.[35] It can be assembled using food-grade *γ*-CD and salt substitute, resulting in body-centered frameworks of $(\gamma\text{-CD})_6$ cubic units. These units easily crystallized

[a] State Key Laboratory of Chemical Engineering, School of Chemical Engineering and Technology, Haihe Laboratory of Sustainable Chemical Transformations, Tianjin University, Tianjin 300072, China. Email: junbo_gong@tju.edu.cn
[b] Beijing National Laboratory for Molecular Science, Key Laboratory of Polymer Chemistry and Physics of Ministry of Education, College of Chemistry and Molecular Engineering, Peking University, Beijing 100871, China
[c] Collaborative Innovation Center of Chemical Science and Engineering. Tianjin 300072, China. Email: chenif@pku.edu.cn

† Supplementary Information available: [details of any supplementary information available should be included here]. See DOI: 10.1039/x0xx00000x

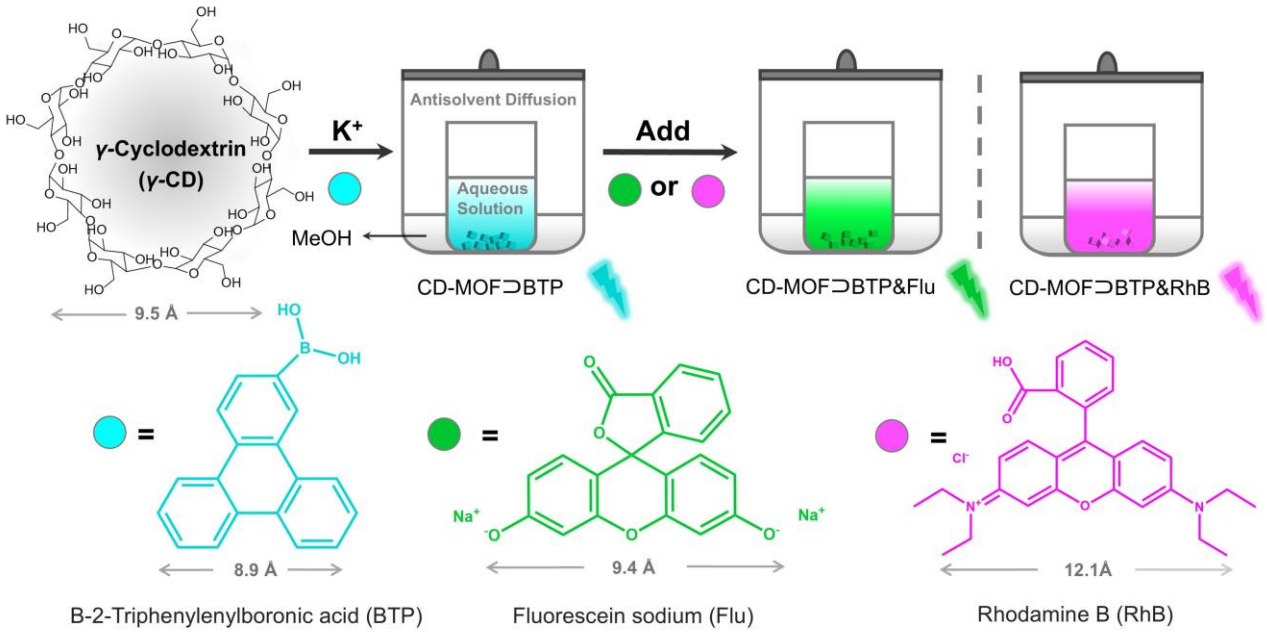

Scheme 1. Schematic illustration of the synthetic process of CD-MOF⊃BTP and the formation of multi-color afterglow.

into millimeter-sized solids. Compared to native γ-CD, CD-MOF demonstrates the ability to encapsulate guest molecules ranging from 0.5 to 2.1 nm in size.[36, 37] Unfortunately, although CD-MOFs have been extensively investigated for various functional materials,[38-40] RTP materials have been scarcely reported.

In this study, we present a universal and efficient strategy to obtain ultralong CD-MOF materials with phosphorescence lifetimes of up to hundreds of milliseconds via in situ encapsulation. B-2-triphenylenylboronic acid (BTP) was selected as the guest molecule due to the following features: (1) The molecular size of BTP matches the cavity of γ-CD, providing the structure prerequisites for effective host-guest complexation. (2) The presence of heteroatoms in BTP enhances intersystem crossing (ISC) efficiency.[41] (3) The boric acid groups can form strong hydrogen bonds with the CD-MOF to minimize nonradiative dissipation. As anticipated, the prepared materials (CD-MOF⊃BTP) exhibit outstanding RTP performance, far superior to the inclusion complexes of γ-CD and BTP. To further validate the universality, derivatives of BTP were rationally selected to construct RTP materials, including triphenylene (TP, non-boronic analogue) and 4,4,5,5-TetraMethyl-2-(3-triphenylen-2-yl-phenyl)-[1,3,2]
dioxaborolane (BMTP, sterically hindered derivative). In addition, by introducing additional fluorescent dyes, such as sodium fluorescein (Flu) and rhodamine B (RhB), into the CD-MOF⊃BTP system, the afterglow colour could be adjusted through Förster-resonance energy transfer (FRET) (Scheme 1).

2. Results and discussion

The preparation of CD-MOF⊃BTP used an in-situ encapsulation strategy as described in previous reports.[35, 42, 43] Briefly, under ambient conditions, methanol vapor was allowed to slowly diffuse into a small glass vial containing γ-CD, KOH, and BTP aqueous solution. Single crystals were obtained after several days at room temperature. (Fig. S1). X-ray powder diffraction data (PXRD) analysis revealed that structural preservation of the CD-MOF framework upon BTP encapsulation (Fig. 1a), indicating that the host framework remains intact even when incorporating guest molecules. Crucially, the intact framework ensures spatial confinement of BTP molecules suppressing aggregation-caused quenching through isolated chromophore arrangement. The UV-Vis diffuse reflectance spectrum of CD-MOF⊃BTP, measured after thorough washing with methanol, exhibited a similar absorption peak to that of pure BTP molecules (Fig. S2). Since γ-CD has no ultraviolet absorption,[44] this indicated that BTP was successfully encapsulated into CD-MOF. As shown in Fig. 1b, the prompt emission spectrum of CD-MOF⊃BTP displays an emission peak at 437 nm, while the delayed spectrum exhibits an emission peak at 487 nm. The time-resolved emission-decay curve revealed a long RTP lifetime of 553 ms for CD-MOF⊃BTP (Fig. 1c), coupled with a quantum yield of 8.19% (Fig. S3). demonstrating its efficient and persistent phosphorescent properties. Moreover, the CD-MOF⊃BTP single crystal exhibited apparent phosphorescence after the UV light was turned off (excitation wavelength of 365 nm), with a cyan afterglow visible to the naked eye for up to 5 s (Fig. 1d, Movie_S1, Movie_S2). For comparison, we recorded the prompt and delayed emission spectra of BTP solid, where the prompt emission spectrum of BTP manifests an emission peak at 382 nm but have no delayed peak (Fig. S4). Furthermore, the time-resolved emission-decay curve showed that millisecond-scale phosphorescence lifetime is absent (Fig. S5). With no doubt, these results confirm that CD-MOF facilitates the stabilization of triplet states, leading to ultralong

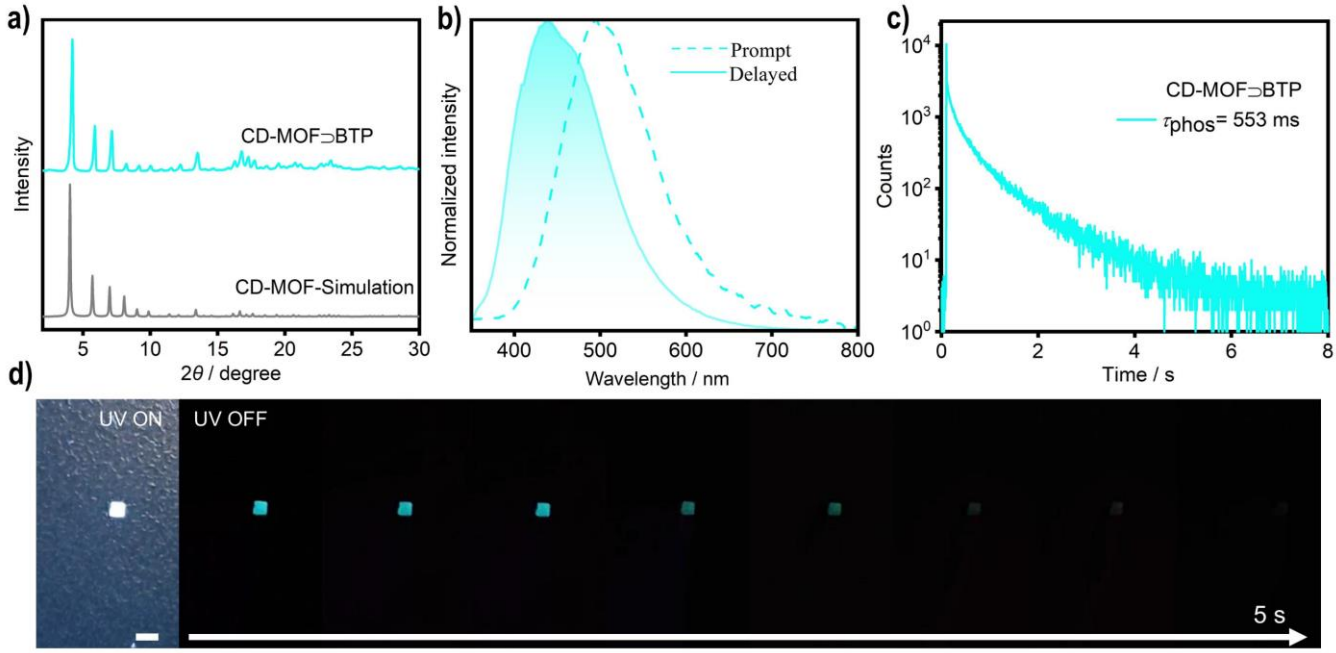

Fig. 1 a) Simulated crystallographic diffraction pattern of CD-MOF (simulated based on available single-crystal structure from the Cambridge structure database, CCDC 2209020). b) Photoluminescence spectra of CD-MOF⊃BTP crystals under ambient conditions (λex = 320 nm). c) Time-resolved decay spectra of CD-MOF⊃BTP under ambient conditions. d) The afterglow photographs of CD-MOF⊃BTP single crystal (the ambient condition is before and after creasing 365 nm UV light). Scar bar: 200 μm.

RTP emission. Finally, we recycled the CD-MOF⊃BTP crystal material for the recrystallization experiment. The recycled crystals maintained identical XRD patterns (Fig. S6) and long-lived performance (Fig. S7), confirming the recyclability of this system.

The cage structure of MOF and cavity structure of CD are known to coexist in CD-MOF (Fig. 2a). In order to demonstrate the advantages of CD-MOF in the preparation of RTP materials, we prepared γ-CD⊃BTP in which only the cavity structure existed and ZIF-8⊃ BTP in which only the cage structure existed. It should be noted that dissolving BTP in aqueous solution requires an alkali, but γ-CD is easy to bond with alkali metals and crystallize. To avoid the effects of alkali metals, γ-CD⊃BTP was prepared using the ball-milling method, with the same amounts of γ-CD and BTP are used CD-MOF⊃BTP. The powder obtained after ball milling was dissolved in water, and the supernatant was collected by filtering after ultrasonic treatment. This solution was then vacuum-dried for two days to yield a powder, which was used for further characterization (Fig. S8). γ-CD⊃BTP also show obvious RTP emission visible to the naked eye after turning off 365 nm UV (Fig. S9, Movie_S3). The prompt emission spectrum displays an emission peak at 375 nm, while the delayed spectrum exhibits an emission peak at 470 nm (Fig. 2b). The time-resolved emission-decay curve showed that the RTP lifetime of γ-CD⊃BTP reached 52 ms (Fig. S10). The isolation of guest molecules by CD has been widely recognized, as its hydrophobic cavities prevent aggregation and restrict nonradiative transitions.[45-47] ZIF-8⊃BTP retained the original framework structure of ZIF-8 (Fig. S11). Spectroscopic data showed that ZIF-8⊃BTP exhibited only prompt emission, with no delayed peak (Fig. S12). By comparison, CD-MOF⊃BTP exhibited a longer phosphorescent lifetime (553 ms vs 52 ms). This phosphorescent lifetime (553 ms) positions itself in the medium–to–upper range of MOF-based phosphorescent materials (Table S1). In the CD-MOF structure, the microenvironment of γ-CD cavity and the framework assembled by γ-CD and potassium ions contribute to forming a rigid and ordered environment. Additionally, the electrostatic interaction between potassium ions and guest molecules effectively suppresses the vibration of the guest molecules and reduces non-radiative transition.[48, 49]

Ulteriorly, in order to demonstrate the feasibility of CD-MOF as a carrier for preparing phosphorescent materials, we investigated two additional guest molecules: TP and its boronic acid-functionalized derivative BMTP (Fig. 2c). Briefly, BT and BMTP were dissolved in $CHCl_3$ to form a clear solution, which was carefully layered on top of the CD-MOF growing solution. [50] CD-MOF⊃TP and CD-MOF⊃BMTP single crystals were obtained by allowing MeOH vapor to slowly diffuse into the layered mixture in three days with PXRD confirming structural integrity of the host framework (Fig. S13-14). CD-MOF⊃TP exhibited no RTP emission due to forbidden ISC transitions in pristine polycyclic aromatic hydrocarbons (Fig. 2e). When a boronic acid group is introduced into triphenylene, it results in a theoretically permitted 1(n, π*) → 3(π, π*) transition for enhancing ISC efficiency. Thus, coupled with the rigid environment provided by CD-MOF, CD-MOF⊃BMTP emitted a blue afterglow upon removing the exciting light, which could be

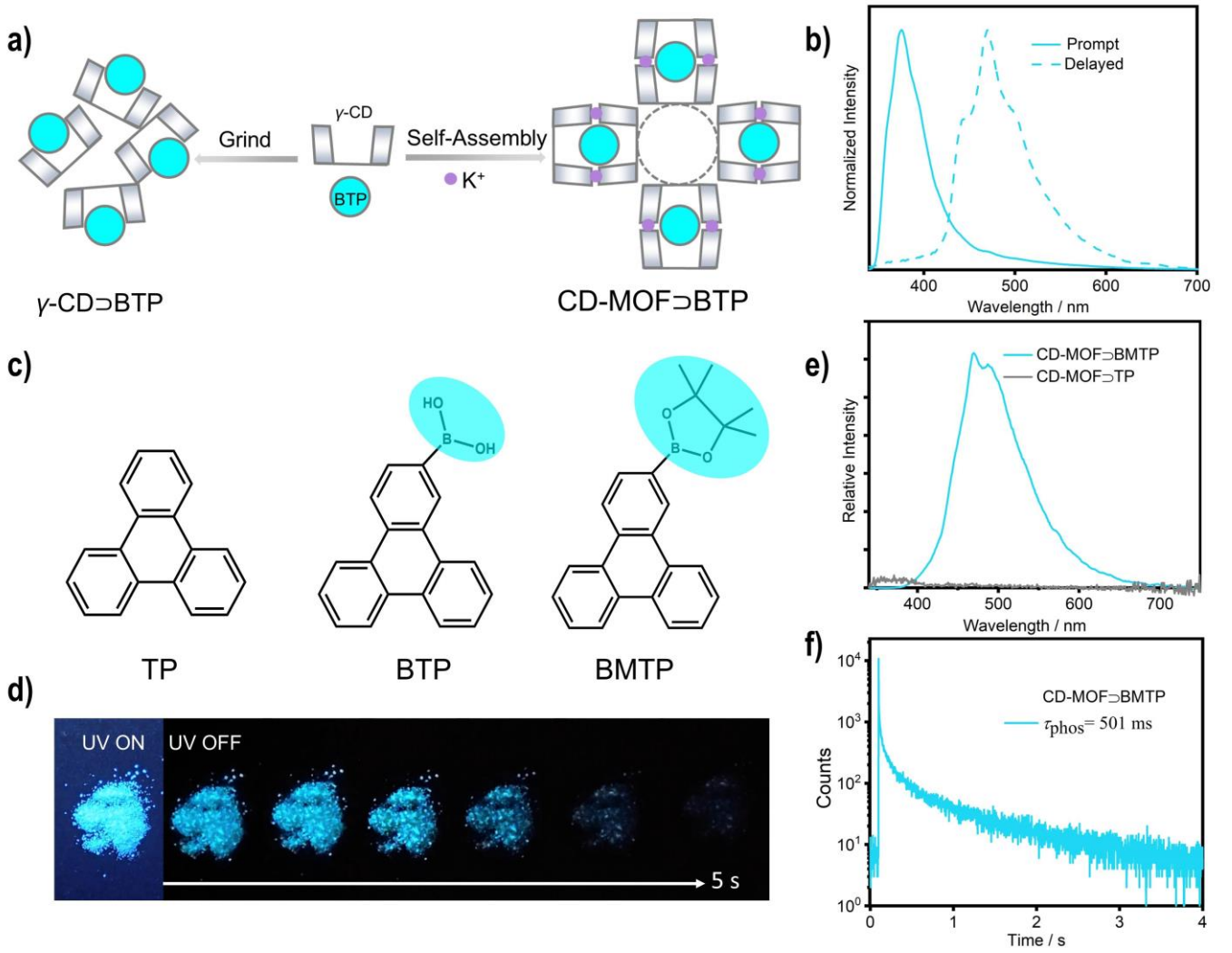

Fig. 2 a) Schematic diagram packing of *γ*-CD⊃BTP and CD-MOF⊃BTP. b) Photoluminescence spectra of *γ*-CD⊃BTP under ambient conditions (λex = 320 nm). c) The chemical structure of BTP derivatives as phosphorescent guests. d) The afterglow photographs of CD-MOF⊃BMTP under ambient condition. e) Phosphorescence spectra of CD-MOF⊃BMTP and CD-MOF⊃TP under ambient conditions. f) Time-resolved decay spectra of CD-MOF⊃BMTP under ambient conditions.

captured by the naked eye and lasted for 5 s (Fig. 2d). Surprisingly, CD-MOF⊃BMTP presented a long lifetime up to 501 ms (Fig. 2f, Movie_S4), which was only shorter than that of CD-MOF⊃BTP (553 ms). This indicates that hydrogen bonding plays a secondary role in RTP enhancement, with heteroatoms effects and spatial confinement being the dominant factors in this study.

To achieve tunable afterglow colors, we implemented a Förster-resonance energy transfer (FRET) strategy by co-encapsulating fluorescent dyes within the CD-MOF⊃BTP system (Fig. 3a). Generally, an efficient FRET process requires the donor and acceptor molecules to be positioned in close proximity and a strong spectral overlap between the donor emission and acceptor absorption spectra.[51] Green dye fluorescein sodium (Flu) and red dye rhodamine B (RhB) were chosen as triplet energy acceptors due to their absorption spectra overlapping significantly with the phosphorescence spectrum of CD-MOF⊃BTP (Fig. S15), which satisfies the premise for energy transfer. Subsequently, materials encapsulated with Flu (CD-MOF⊃BTP&Flu) and RhB (CD-MOF⊃BTP&RhB) were prepared and characterized by X-ray powder diffraction and ultraviolet absorption (Fig. S16-19). As the concentration of acceptor dyes increased, CD-MOF⊃BTP&Flu and CD-MOF⊃BTP&RhB exhibited gradual color transformations ranging from blue to green or pink, respectively (Fig. 3e). Meanwhile, the intensity of the donors' phosphorescence peak became weaker, while the intensity of the acceptors' delayed fluorescence peak of the receptor became more robust in the phosphorescence spectrum, which implied the high efficiency energy transfer from the donor to the acceptor (Fig. 3b-c). Impressively, when the molar ratio of the donor and acceptor was 10:1, CD-MOF⊃BTP&Flu exhibited green luminescence (τphos = 415 ms) upon removing the exciting light (Movie_S5). When the donor and acceptor molar ratio is 5:1, CD-MOF⊃BTP&RhB exhibited pink luminescence (τphos = 430 ms) upon removing the exciting light (Fig. 3d, Movie_S6). However, with the increase of

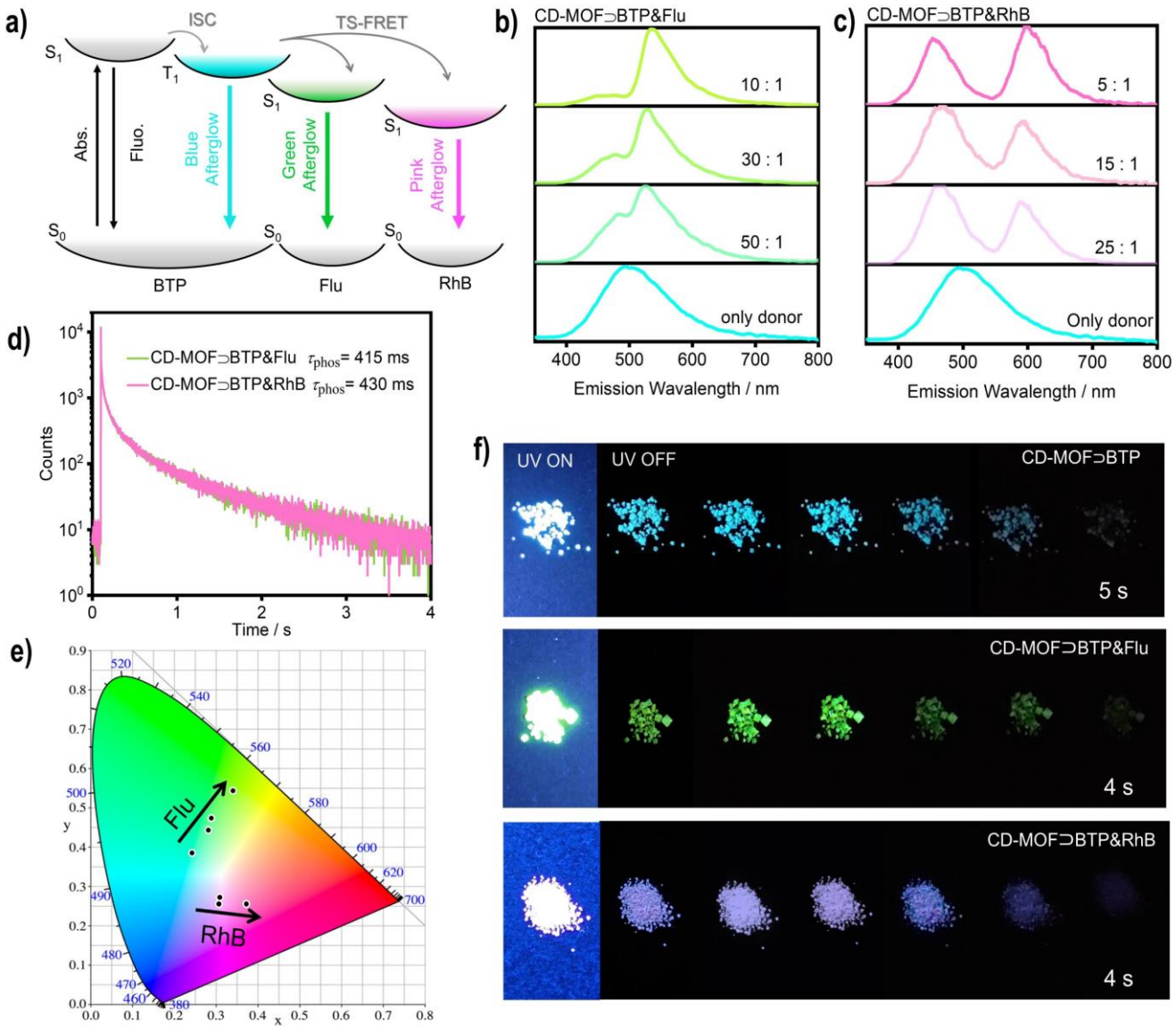

Fig. 3 Luminous properties of CD-MOF⊃BTP&acceptor-dyes. a) Simplified Jablonski diagram for ultralong phosphorescence and full-color energy transfer process. b-c) Delayed emission spectra of CD-MOF⊃BTP with different acceptor concentrations under ambient conditions (left is CD-MOF⊃BTP&Flu, right is CD-MOF⊃BTP&RhB). d) Time-resolved decay spectra of CD-MOF⊃BTP&acceptor under ambient conditions (CD-MOF⊃BTP&Flu, the molar ratio of BTP to Flu ([TP]:[Flu]) is 10:1; CD-MOF⊃BTP&RhB, the molar ratio of BTP to RhB ([TP]:[RhB]) is 25:1 (λex = 320 nm). e) CIE 1931 chromaticity diagram of afterglow color changes when CD-MOF⊃BTP was doped with different acceptor concentrations. f) Full-color afterglow photographs of CD-MOF⊃BTP, CD-MOF⊃BTP&Flu ([TP]:[Flu] is 10:1) and CD-MOF⊃BTP&RhB ([TP]:[RhB] is 25:1).

acceptor concentrations, the afterglow lifetime was significantly reduced (Fig. S20-21). The significant afterglow quenching might result that high acceptor concentrations lead to quenching of ling-lived triplet excitons.

Leveraging the tunable phosphorescence color and lifetime of the materials, we fabricated diverse luminescence patterns using MOF powders and custom molds. As depicted in Fig. 4a, a "dolphin" pattern was created using CD-MOF⊃BTP powder, which exhibited a vivid cyan afterglow lasting over 4 seconds upon UV light cessation. For information encryption, we designed a text-based pattern where the letters "T" and "U" were filled with CD-MOF⊃BTP powder, while a second "J" was filled with the green-emitting CD-MOF⊃BTP&Flu (the molar ratio of BTP to Flu ([TP]:[Flu]) is 10:1). The different colored monograms can be observed through turning off the UV lamp. This gradual change indicates the potential for use in anticounterfeiting systems. To further illustrate the information encryption capability, an “888” pattern was designed, where the blue, green, and pink emissive parts observed under 365 nm UV lamp correspond to the visible emission of CD-MOF⊃BTP, CD-MOF⊃BTP&Flu ([TP]:[Flu] is 10:1) and CD-MOF⊃BTP&RhB ([TP]:[RhB] is 1:1), respectively. Under UV light, the pattern

displayed "888", but upon UV removal, it immediately delivers an invalid binary code. Upon the UV light excitation,

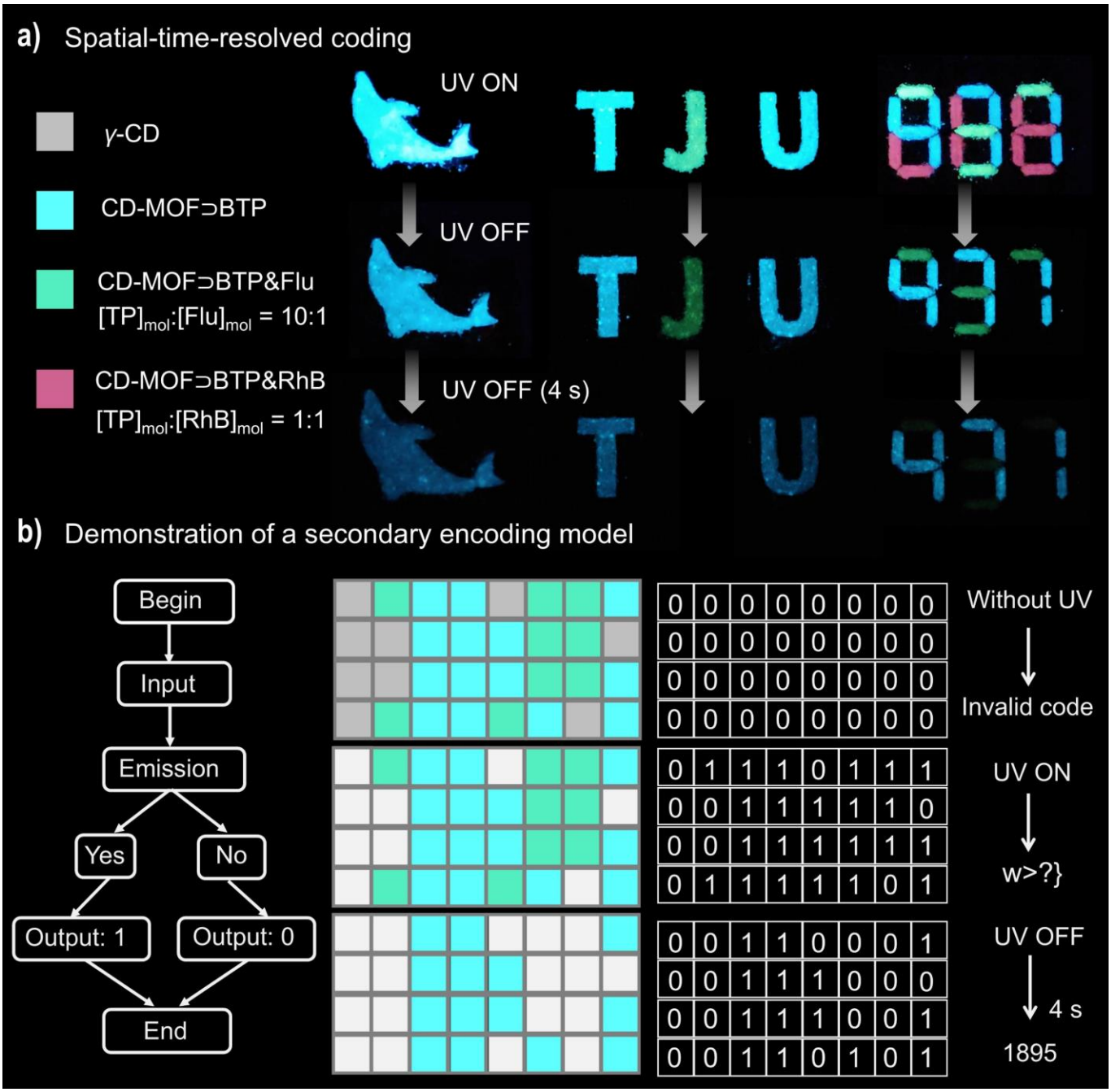

Fig. 4 a) Potential applications. Display, multilevel anticounterfeiting and information encryption shown by the patterns of "dolphin", "TJU" and "888" taken at 365 nm UV "on" and "off" condition fabricated based on MOFs with different emission color and lifetime. b) Optical logic gate model based on the time-resolved anticounterfeiting system, which changes the binary code into ASCII code to obtain information.

transformed to "937" and gradually evolved to "471" due to the differential decay rates of the phosphorescent materials (Fig. 4a). Finally, we designed a secondary encoding model according to the adjustable phosphor lifetime (Fig. 4b). Two color MOFs materials and non-emissive *γ*-CD were selectively filled into the groove to enable a dot-matrix pattern (4 × 8). We can define that if the dot is emissive, then the output is "1"; otherwise, the output is "0". A uniform pattern is observed under sunlight and dot-matrix pattern given a misleading code of "w>?}" by transforming the binary code to ASCII (American Standard Code for Information Interchange) code. When removing the UV light, the correct code will be given, and the code is deciphered as "1895" by directly translating the binary code to ASCII code. The above results indicate phosphorescence MOF materials potential applications in advanced display, anticounterfeiting, and information encryption.

3. Conclusions

In summary, this work reported an assembly system based on environment friendly CD-MOF as a host and B-2-triphenylenylboronic acid as the guest. This system exhibits a long lifetime and excellent phosphorescence quantum yield of 553 ms and 8.19 %, respectively. Furthermore, doping with several commercial dyes, full-color afterglow emissions with an ultralong RTP are realized through energy transfer. With these high-performance doped systems, display, multilevel anticounterfeiting and information encryption are successfully implemented. This work demonstrates the advantages of supramolecular macrocycle-based crystalline materials for RTP materials, and provides a simple, universal platform for future.

Author contributions

Jiayin Zhang: Writing–original draft, Methodology, Investigation, Formal analysis, Data curation, Conceptualization. **Jiaxuan Tang**: Investigation, Formal analysis, Data curation. **Yongsheng Zhang**: Methodology, Investigation, Data curation. **Yifu Chen**: Supervision, Funding acquisition. **Junbo Gong**: Supervision, Resources, Funding acquisition.

Conflicts of interest

There are no conflicts to declare.

Data availability

The data that support the findings of this study are available in the ESI† and from the corresponding author upon request.

Acknowledgements

This work was supported by the National Natural Science Foundation of China (22478285, 22378302 and 22405011), Tianjin Youth Science and Technology Talent Project (QN20230220), and the National Science Foundation of Beijing City (2244091) for financial support. Y.C. additionally acknowledges the funding of Boya Postdoctoral Fellowship at Peking University and BMS Junior Fellow Program.

Notes and references

1. C. J. Fischer, A. Gafni, D. G. Steel and J. A. Schauerte, *J. Am. Chem. Soc.,* **2002**, 124, 10359-10366.
2. G. Zhang, J. Chen, S. J. Payne, S. E. Kooi, J. N. Demas and C. L. Fraser, *J. Am. Chem. Soc.,* **2007**, 129, 8942-8943.
3. M. A. Baldo, D. F. O'Brien, Y. You, A. Shoustikov, S. Sibley, M. E. Thompson and S. R. Forrest, *Nature*, **1998**, 395, 151-154.
4. Z. Wang, J. J. Pan, X. Q. Chen, M. Y. Li and M. Pan, *Chemical Engineering Journal,* **2025**, 509.
5. Z. Wang, C. Q. Li, J. T. Mo and M. Pan, *Aggregate*, **2025**, e696.
6. Z. Wang, J. T. Mo, J. J. Pan and M. Pan, *Advanced Functional Materials*, **2023**, 3, 2300021.
7. H. Sun and L. L. Zhu, *Aggregate*, **2023**, 4, e253.
8. Kenry, C. J. Chen and B. Liu, *Nature Communications*, **2019**, 10, 2111.
9. S. M. A. Fateminia, Z. Mao, S. D. Xu, Z. Y. Yang, Z. G. Chi and B. Liu, *Angew. Chem., Int. Ed.,* **2017**, 56, 12160-12164.
10. L. Gu, H. W. Wu, H. L. Ma, W. P. Ye, W. Y. Jia, H. Wang, H. Z. Chen, N. Zhang, D. D. Wang, C. Qian, Z. F. An, W. Huang and Y. L. Zhao, *Nature Communications,* **2020**, 11, 944.
11. Z. Z. Li, Q. Yue, Y. He and H. C. Zhang, *ACS Appl. Mater. Interfaces,* **2024**, 16, 25415-25421.
12. D. Li, Y. J. Yang, J. Yang, M. M. Fang, B. Z. Tang and Z. Li, *Nature Communications,* **2022**, 13, 347.
13. Y. Y. Gong, G. Chen, Q. Peng, W. Z. Yuan, Y. J. Xie, S. H. Li, Y. M. Zhang and B. Z. Tang, *Advanced Materials,* **2015**, 27, 6195-6201.
14. H. R. Wang, Q. Y. Li, J. Y. Zhang, H. K. Zhang, Y. H. Shu, Z. Zhao, W. Jiang, L. L. Du, D. L. Phillips, J. W. Y. Lam, H. H. Y. Sung, I. D. Williams, R. Lu and B. Z. Tang, *J. Am. Chem. Soc.,* **2021**, 143, 9468-9477.
15. J. Yang, X. Zhen, B. Wang, X. M. Gao, Z. C. Ren, J. Q. Wang, Y. J. Xie, J. R. Li, Q. Peng, K. Y. Pu and Z. Li, *Nature Communications,* **2018**, 9, 840.
16. Z. Wang, J. J. Liu, S. Y. Yin, M. Y. Li, Y. J. Hou, D. Wang, J. T. Mo and G. Chen, *Advanced Functional Materials,* **2023**, 33, 2212985.
17. Z. Wang, J. J. Liu, M. Y. Li and G. Chen, *Chemical Engineering Journal,* **2023**, 462, 142154.
18. Y. Xie, G. T. Sun, J. W. Li and L. N. Sun, Advanced Functional Materials, **2023**, 33, 2303663.
19. J. B. Chen, R. R. Sun, W. J. Yang, F. F. Xing, X. L. Yu and L. N. Sun, *J Mater Chem C*, **2025**, 13, 1157-1164.
20. J. T. Mo and Z. Wang, *Chinese Chemical Letters*, **2024**, 35, 9, 109360.
21. D. Li, Z. J. Liu, M. M. Fang, J. Yang, B. Z. Tang and Z. Li, *Acs Nano*, **2023**, 17, 12895-12902.
22. D. F. Li, F. F. Lu, J. Wang, W. D. Hu, X. M. Cao, X. Ma and H. Tian, *J. Am. Chem. Soc.,* **2018**, 140, 1916-1923.
23. W. L. Zhou, Y. Chen, Q. L. Yu, H. Y. Zhang, Z. X. Liu, X. Y. Dai, J. J. Li and Y. Liu, *Nature Communications*, **2020**, 11, 4655.
24. X. K. Ma, W. Zhang, Z. X. Liu, H. Y. Zhang, B. Zhang and Y. Liu, *Advanced Materials*, **2021**, 33, 2007476.
25. Z. C. Liu, S. K. M. Nalluri and J. F. Stoddart, *Chem. Soc. Rev.*, **2017**, 46, 2459-2478.
26. T. Jiang, G. J. Qu, J. Wang, X. Ma and H. Tian, *Chemical Science*, **2020**, 11, 3531-3537.
27. Z. X. Liu and Y. Liu, *Chem. Soc. Rev.*, **2022**, 51, 4786-4827.
28. A. M. de la Peña, M. C. Mahedero and A. B. Sánchez, *Analusis*, **2000**, 28, 670-678.
29. G. Crini, *Chem. Rev.*, **2014**, 114, 10940-10975.
30. N. J. Turro, J. D. Bolt, Y. Kuroda and I. Tabushi, *Photochem. Photobiol.*, **2008**, 35, 69-72.
31. X. L. Zhou, X. Zhao, X. Bai, Q. W. Cheng and Y. Liu, *Advanced Functional Materials*, **2024**, 34, 2400898.
32. I. Roy and J. F. Stoddart, *Acc Chem Res*, **2021**, 54, 1440-1453.
33. Y. J. Ma, X. Y. Fang, G. W. Xiao and D. P. Yan, *Angew. Chem., Int. Ed.*, **2022**, 61, e202114100.
34. X. G. Yang, X. Q. Lin, Y. B. Zhao, Y. S. Zhao and D. P. Yan, *Angew. Chem., Int. Ed.*, **2017**, 56, 7853-7857.
35. R. A. Smaldone, R. S. Forgan, H. Furukawa, J. J. Gassensmith, A. M. Slawin, O. M. Yaghi and J. F. Stoddart, *Angew. Chem. Int. Ed.*, **2010**, 49, 8630-8634.
36. Y. Chen, B. Yu, Y. Cui, S. Xu and J. Gong, *Chem. Mater.*, **2019**, 31, 1289-1295.

37. L. Y. Hu, K. Li, W. L. Shang, X. F. Zhu and M. H. Liu, *Angew. Chem., Int. Ed.*, **2020**, 59, 4953-4958.
38. R. N. Zhao, B. W. Zhu, Y. Xu, S. F. Yu, W. J. Wang, D. H. Liu and J. N. Hu, *Carbohydrate Polymers*, **2023**, 319, 121198.
39. T. Rajkumar, D. Kukkar, K. H. Kim, J. R. Sohn and A. Deep, *Journal of Industrial and Engineering Chemistry*, **2019**, 72, 50-66.
40. Y. Y. Peng, Y. Z. Lei, J. Luo, X. W. Hu, F. W. Sun, Y. H. Yang, M. S. Guo and T. Cai, *Chemical Engineering Journal*, **2024**, 479, 147654.
41. E.-S. M. A. LOWER S K, *Chem. Rev.*, **1966**, 66, 199-241.
42. R. S. Forgan, R. A. Smaldone, J. J. Gassensmith, H. Furukawa, D. B. Cordes, Q. Li, C. E. Wilmer, Y. Y. Botros, R. Q. Snurr, A. M. Slawin and J. F. Stoddart, *J. Am. Chem. Soc.*, **2012**, 134, 406-417.
43. J. Zhang, Y. Chen, Y. M. Zhang and J. Gong, *Chemistry – A European Journal*, **2024**, 30, e202402068.
44. Z. i. Yoshida, H. Takekuma, S. i. Takekuma and Y. Matsubara, *Angew. Chem., Int. Ed.*, **1994**, 33, 1597-1599.
45. X.-K. Ma, Q. Cheng, X. Zhou and Y. Liu, *JACS Au*, **2023**, 3, 2036-2043.
46. J. Wang, X. Y. Lou, J. Tang and Y. W. Yang, *J. Polym. Sci.*, **2023**, 61, 903-911.
47. H. Zhu, L. Y. Chen, B. Sun, M. B. Wang, H. Li, J. F. Stoddart and F. H. Huang, *Nature Reviews Chemistry*, **2023**, 7, 768-782.
48. Z. H. Gao, B. Y. Xu, T. J. Zhang, Z. Liu, W. G. Zhang, X. Sun, Y. Liu, X. Wang, Z. F. Wang, Y. L. Yan, F. Q. Hu, X. G. Meng and Y. S. Zhao, *Angew. Chem., Int. Ed.*, **2020**, 59, 19060-19064.
49. D. Venkatakrishnarao, M. A. Mohiddon, N. Chandrasekhar and R. Chandrasekar, *Advanced Optical Materials*, **2015**, 3, 1035-1040.
50. X. L. Yang, Z. Y. Yang, R. Shao, R. F. Guan, S. L. Dong and M. H. Xie, *Advanced Materials*, **2023**, 35, 2304046.
51. L. Wu, C. Huang, B. P. Emery, A. C. Sedgwick, S. D. Bull, X.-P. He, H. Tian, J. Yoon, J. L. Sessler and T. D. James, *Chem. Soc. Rev.*, **2020**, 49, 5110-5139.

Data availability

The data that support the findings of this study are available in the ESI† and from the corresponding author upon request.